




Article

Effect of LULC Changes on Annual Water Yield in the Urban Section of the Chili River, Arequipa, Using the InVEST Model

Lorenzo Carrasco-Valencia ¹, Karla Vilca-Campana ¹, Carla Iruri-Ramos ¹, Berly Cárdenas-Pillco ¹, Alfredo Ollero ² and Andrea Chanove-Manrique ^{1,*}

¹ Facultad de Arquitectura e Ingenierías Civil y del Ambiente, Universidad Católica de Santa María, Arequipa 040101, Peru; 71629417@ucsm.edu.pe (L.C.-V.); 76354812@ucsm.edu.pe (K.V.-C.); ciruri@ucsm.edu.pe (C.I.-R.); bcardenas@ucsm.edu.pe (B.C.-P.)

² Departamento de Geografía y Ordenación del Territorio, Instituto de Ciencias Ambientales de Aragón (IUCA), Universidad de Zaragoza, 50009 Zaragoza, Spain; aollero@unizar.es

* Correspondence: achanove@ucsm.edu.pe

Abstract: Arequipa is a semi-desert city located in southern Peru which depends on the Chili River as its only water source. During recent years, this city has increased its number of inhabitants significantly as a result of internal migratory flows and population growth. Because of this, the city has undergone a rapid urbanization process which has increased the urban areas near the river and caused the destruction of agricultural areas, as well as their native vegetation. This change in land use can be quantified through satellite image analysis across many years, but as noted, there are no studies on its impact on water yield (WY) in the urban section of the river. Now, by using the Integrated Valuation of Ecosystem Services and Compensation (InVEST) model, which allows the WY of the study area to be evaluated in millimeters and cubic meters by introducing a series of variables, such as precipitation, reference evapotranspiration and types of land use classes, among others, it is possible to determine that the WY from the study area was 1,743,414 m³ in 1984 and 1,323,792 m³ in 2022; the urban area is the type of land use with the highest increase with respect to its percentage contribution to the WY, going from 30.43% to 49.62% between 1984 and 2022, respectively. The increase in urban area mitigated the loss of total WY, explained by a higher percentage runoff rate, surface flow and drainage problems in the study area.

Keywords: ecosystem services; urban river; land use/land cover; evapotranspiration; precipitation; water balance



Citation: Carrasco-Valencia, L.; Vilca-Campana, K.; Iruri-Ramos, C.; Cárdenas-Pillco, B.; Ollero, A.; Chanove-Manrique, A. Effect of LULC Changes on Annual Water Yield in the Urban Section of the Chili River, Arequipa, Using the InVEST Model. *Water* **2024**, *16*, 664. <https://doi.org/10.3390/w16050664>

Academic Editors: Bommana Krishnappan and Rui Manuel Vitor Cortes

Received: 12 December 2023

Revised: 10 February 2024

Accepted: 15 February 2024

Published: 24 February 2024



Copyright: © 2024 by the authors. Licensee MDPI, Basel, Switzerland. This article is an open access article distributed under the terms and conditions of the Creative Commons Attribution (CC BY) license (<https://creativecommons.org/licenses/by/4.0/>).

1. Introduction

Urban rivers are ecological corridors that maintain landscape connectivity, protect biodiversity and provide a multiplicity of ecosystem services (ESs) for human health and human well-being [1–3], increasing cities' global levels of resilience against climate change [4,5].

Over the years, population growth, climate change impacts and the change in land use [3,6,7] have generated a larger area composed of waterproof surfaces, which translates into limited humidity exchange, temperature increase [8] and a negative impact on the ESs related to urban rivers as hydric resources. Deforestation and agricultural land expansion cause an increase in annual runoff, evapotranspiration, river flow, groundwater depletion and lateral flow [9].

Water yield (WY) is an ES that plays a key role in ecosystem management and hydrological balance. It also contributes to society's well-being and guarantees the development of agriculture irrigation and the industrial development of diverse activities [10,11]. Water yield represents precipitation distribution based on vegetation, helping to retain humidity and regulate runoff [12–14].

WY depends on evapotranspiration (AET), mean annual precipitation (MAP) and land use/land cover (LULC) [12–14]. It is generally understood that increasing an ES would be usually beneficial; however, in the case of WY, a negative increase implies the loss of capacity to regulate the balance of the hydrological cycle, given the alteration in one of the key components such as vegetation cover. In the absence of vegetation, water—which would commonly follow the route of evapotranspiration and infiltration—decreases, thus increasing the volume of surface water [14,15]. Likewise, immediately after rain events, surface water flows would increase, generating soil erosion and flooding, and therefore a low contribution to the underground hydrological system [14,16], which increases the severity of droughts, especially in arid regions where rainfall is scarce and seasonal [17].

It is necessary to take measures in order to protect watershed and prevent WY depletion [18]. Consequently, the WY must be evaluated in a quantitative form and visualized in maps that allow for the explanation of changes in land use/land cover (LULC) in relation to its change. WY models allow us to predict ES distribution patterns in relation to changes in LULC, so they can be used as support for territorial planning [14]; however, it is essential to consider the social context, so they can also constitute a tool for ecological education.

To evaluate WY, the Integrated Valuation of Environmental Services and Compensations (InVEST) is widely used [6,9,18–20]. This model allows for the simulation of water spatial distribution according to the water balance method by using maps with biophysical attributes for each coverage defined for each territory pixel [6,14,18] in such a way that it spatially explores which transformations in the ecosystem lead to changes in this ES received by communities [21]. These evaluations represent important tools for effective protection and management of water resources [9,22], as well as for an adequate relationship between human growth and WY through the articulation of production spaces, housing and ecological value to achieve cities' sustainable development and human well-being [6,23]. Consequently, the measurement of the WY and the LULC changes through InVEST will contribute to achieve the sustainable development goals [24] aimed at the care of water resources, the protection of ecosystems and the development of sustainable communities, especially in cities with a clear trend toward urban growth, where the loss of natural ecosystems generates environmental and economic damage [14] that threatens the quality of life of the population.

Nowadays, InVEST represents a reliable and practical model [18], which is widely used to evaluate ecosystem services due it is expression of maps [6,25]. The spatialization of the output results facilitates the identification of important areas of ESs, such as the evaluation of carbon storage and sequestration [26,27], risk assessment and habitat quality [28,29], soil erosion and conservation [30], flood risks [31,32], water yield [33,34] and urban cooling [35], among others. It is important to consider that this model does not make a distinction between surface and underground flow, but it assumes that all of the water from a pixel reaches the point of interest through one of these routes [21].

Diverse studies have been carried out to evaluate WY by using the InVEST model. The WY studies consider many factors, such as change in LULC, annual precipitation and AET. It is noted that there is a positive relationship between precipitation and WY [36], while changes in land cover show different impacts that must be evaluated [37,38]. In addition to this, there are other factors involved in WY with less influence, such as the topographic and geological configuration of basins [39].

Also, different relations, such as areas with greater vegetation that tend to decrease their water yield due to their capacity to provide more humidity to the soil, must also be taken into consideration [9,40], and if the forest and agricultural areas increase, the water yield tends to decrease [7]. Another factor to be considered refers to the following relationship: the higher the level of coverage transformation, the higher the increase in water yield [14]. There are also studies that analyze compensations and synergies for different land use scenarios, evaluating economic growth and ecological conservation, combining them based on factors such as carbon capture, soil retention capacity, WY and

nutrient export, where compensation would decrease in the carbon capture and nutrient export of the ES significantly, even in the ecological conservation scenario at the end [37].

Having objective figures expressed in cubic meters on the annual water yield of an area not only facilitates the service economic evaluations, but it also becomes a reference for future investment projects on the proper exploitation of this resource.

In spite of the anthropogenic pressure on the ecological corridor of the Chili River [41], due to processes referring to rapid urbanization and economic development that result in a deficit of green areas, loss of intra-urban agricultural areas and decrease in the ESs provided by the river to the city [42], the river's hydrographic basin does not have any studies that quantify the WY in its urban section.

Currently, no study exists that addresses the ecosystem service of water yield in our country, which is necessary for future conservation projects to evaluate the effects of land use change in urban ecosystems, as well as helping future environmental economic valuation studies. This paper would be the first study that contributes to modeling the analysis of another urban river. In addition, to determine the ecosystem service's performance, INVEST is applied, which is a modern and practical model applied in some studies [43] and is an important tool for the analysis of the effects on ecosystem services. This study is differentiated by the model's application to an arid region with the presence of a river that crosses a constantly growing urban area, emphasizing the direct relationship between the WY ecosystem service and land cover change. More of these studies are needed to evaluate WY in an ecosystem.

Therefore, given the importance of this river as a main source of urban and rural water supply for the city and the uncontrollable trend toward greater urbanization of the basin, the objective of this study focuses on evaluating the dynamics of change in land use and vegetation between the years 1984 and 2022 and aims to analyze whether this affects or modifies the WY in the urban section of the river. In this way, its results will contribute to a greater rationalization for future actions corresponding to ES management and to better decision making regarding the most adequate planning and management of the hydric resource and land use.

2. Materials and Methods

2.1. Study Area

The Chili River originates from the confluence of Blanco and Sumbay Rivers. It also belongs to the Quilca-Chili basin that extends within the Arequipa region [41]. The basin is located on the western side of the Andes Mountains and belongs to the hydrographic region of the Pacific Ocean. The Quilca-Chili basin is made up of 11 hydrographic units. The study area is part of the Medio Quilca-Vitor-Chili hydrographic unit, which has a total area of 2334.60 km². This unit includes the extension of the Chili River, which is 88.2 km [44], and the research study area includes the urban section with an extension of 39.7 km (Figure 1).

The urban section of the Chili River was previously defined in a study carried out by [45] according to Durán, Pons and Serrano [46] from the application of the criterion for standardized distances around the riverbeds, adjusted to the existing urban legislation for the case study [47]. Subsequently, two types of urban sections were differentiated; first, the "intra-urban" ones that have urban uses on both banks, and second, the "peri-urban" ones that have urban uses on a single bank (Figure 1). It is considered that the fluvial section must be urban whenever there is material urban coverage in a 100 m range measured from the banks of the river and in the entire perimeter surrounding it. Isolated urban infrastructures were discriminated against, so urban developments whose surfaces are greater than 20 ha are considered and contribute to the consolidation and functionality of the urban frame.

Arequipa is the second largest city of Peru in economic and population terms, so it is one of the most important urban zones on a national scale [47]. The city grows under a monocentric development model which is combined with an explosive territorial

expansion that has led to indiscriminate urban growth, increasing urban fragmentation and disarticulation with existing natural ecosystems [47]. The Chili River runs through the city, acting as an important axis in its territorial configuration. All along its route, it borders urban, historical and agricultural areas. Its basin provides urban and rural water which allows for the development of energy and agricultural activities [48], and it also represents an emblematic place for citizens [49].

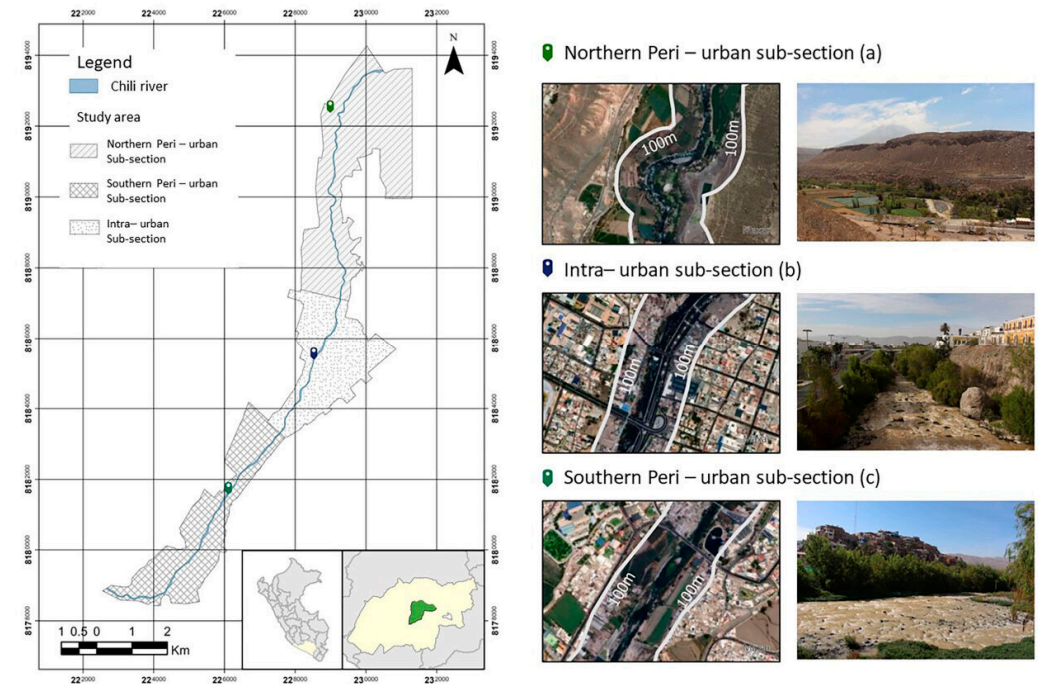


Figure 1. Map of the urban basin of Chili River and its defined sub-sections [45].

2.2. Model Inputs

The methodology flow chart (Figure 2) was adapted from the study conducted by [3]. The same procedure was applied for both years, 1984 and 2022, with the inputs of the root boundary layer depth, the study area and the available water content for plants being constant parameters for both years when calculating water performance.

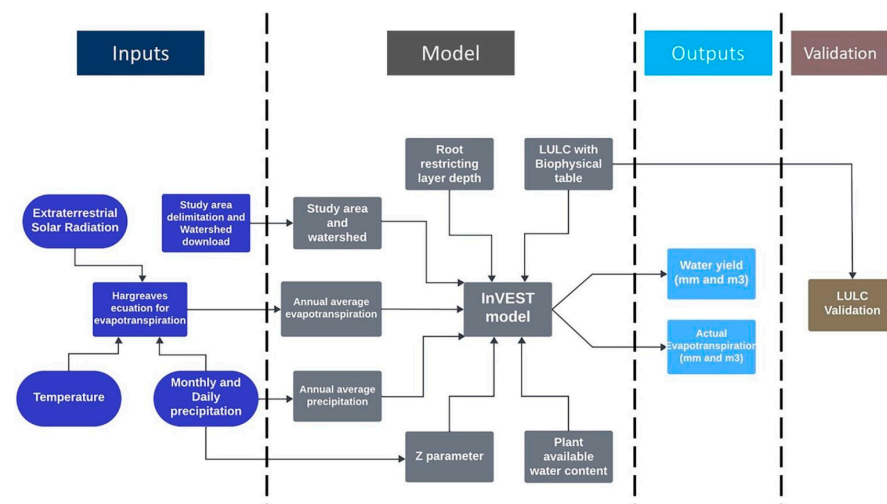


Figure 2. Flow diagram to calculate water yield in the urban area of Chili River using the InVEST AWY Model.

Table 1 shows the data from those inputs as well as their respective sources. Some inputs such as Evapotranspiration and Available water content needed to be processed via equations.

Table 1. Data inventory for model inputs.

Model Inputs	Data Source	Note
Annual precipitation	Precipitation data from Senamhi, La Pampilla meteorological station.	
Annual reference evapotranspiration	Temperature and precipitation data from Senamhi, La Pampilla meteorological station; solar radiation data from Peruvian Association of Solar Energy and Environment.	Based on the Hargreaves equation
LULC rasters	Sentinel-2 from Copernicus program and Landsat 5 from Earth Explorer. Ecological and economical zoning of Arequipa (2017).	
Available water content for plants raster	International Soil Reference and Information Center (ISRIC) SoilGrids 2017 AWC data.	Application of the Hengl equation
Root-restricting layer depth raster	Global Soil Information Grid platform provided by ISRIC.	
Biophysical table	FAO, InVEST user's guide.	
Z parameter	Precipitation data from Senamhi, La Pampilla meteorological station.	

2.2.1. Annual Precipitation and Annual Reference Evapotranspiration

Daily values of precipitation and maximum and minimum temperature values for the years 1984 and 2022 were obtained from the Servicio Nacional de Meteorología e Hidrología del Perú (SENAMHI) from the Pampilla station (the closest to the study area and the only one that is valid since the first year for comparison), and also, monthly average values were calculated [9]. These years were chosen due to their time and distance in order to obtain a better change in land use at the moment of analyzing the effect produced by this variable in the WY, and also because in these years, the number of precipitation events (greater than 1 mm per day) were the same in both years (18 events) which allowed us to make the Z parameter into a constant.

The precipitation rasters were created in QGIS by forming a polygon cut with the study zone as a mask and modifying the attribute table in order to create a field containing the annual precipitation (adding the monthly ones) in the zone and subsequently, rasterizing the polygon using that field as a value for marking.

The reference evapotranspiration varies with elevation, latitude, humidity and slope aspect. There are many methodologies which range in data requirements and precision. You can calculate the reference ET by developing monthly average grids of precipitation and maximum and minimum temperatures. Temperature and precipitation data are often available from regional charts, direct measurements or national or global datasets (such as WorldClim). Radiation data, on the other hand, are far more expensive to measure directly but can be reliably estimated from online tools, tables or equations [21].

The annual reference evapotranspiration was obtained by using the modified Hargreaves equation using the monthly precipitation values (P) in mm/month, the monthly averages of daily maximum and minimum temperatures (T_{av}) in degrees Celsius, the difference among these averages (TD) and the solar radiation value expressed in $MJ/m^2.d$ (RA) [21].

Hargreaves equation is modified as follows:

$$ETo = 0.0013 \times 0.408 \times RA \times (Tav + 17) \cdot (TD - 0.0123 \times P)^{0.76} \quad (1)$$

where ETo is expressed in mm/month.

A strong recommendation that the input evapotranspiration raster be based on the same precipitation data that are entered into the model was taken into account too [24], so there is more consistency and reliability in the results.

The solar radiation data were obtained based on a study performed by the Asociación Peruana de Energía Solar y del Ambiente in 2015 [50]. These data were expressed in $KWh/m^2.d$ and had to be converted into $MJ/m^2.d$ in order to be applicable to the equation.

2.2.2. Land Use/Land Cover

To create the land use raster, satellite images with a cloud cover near zero in each year to be compared were downloaded. The 1984 satellite image was also downloaded on the Earth Explorer platform and the Landsat 5 satellite, since it was the most advanced at that time and had a 30×30 m resolution, while the 2022 satellite images were downloaded through the Copernicus program and the Sentinel-2 satellite, which has a 10×10 m resolution. These satellite images were cut using the study area in a vector format as a template.

Following this procedure, 5 main types of land use classes were identified through the use of level II of Corine Land Cover classification; these were urban fabric (UF), heterogeneous agricultural areas (HAA), forest (F), open spaces with little or no vegetation (OS) and inland waters (IW). According to the Arequipa's ecological and economical zoning in vector format [51], the open spaces category was sub-divided into open spaces 1 (OS1) referring to Cardonal (area populated with cacti), and open spaces 2 (OS2) referring to Puyal (area populated with puyas, *Puyoideae genus*), resulting in 6 types of land use classes as Table 2 shows. The forest (F) category represents riparian forest, located on the riverside hills, and the inland waters (IW) category refers to the Chili River.

Table 2. Land use classes found in the study area according to the Corine Land Cover classification.

LULC Classes	Abbreviation
Inland waters (river)	IW
Forest (riparian forest)	F
Open spaces 1 (Cardonal)	OS1
Heterogeneous agricultural areas (agriculture)	HAA
Urban fabric (urban)	UF
Open spaces 2 (Puyal)	OS2

Note: Adapted from [52].

Using the SCP plugin tool, ROI polygons were created with reference to the satellite images that covered these different types of land use classes as accurately as possible until they covered the entire study area. After this, a mosaic was created using the 6 land use classes. These 6 layers were combined into one and then the rasterization process with a 10×10 m resolution was applied to finally obtain classified land use rasters that would be applied in the model [45].

Since these are average values over several years which also only vary significantly with latitude changes, these have been applied as a constant variable for both 1984 and 2022.

Subsequently, evapotranspiration rasters were created by using the same method used for precipitation rasters.

2.2.3. Available Water Content for Plants

These data were downloaded from the ISRIC website and were a constant parameter for both study years. The data consist of the water fraction that can be stored in the soil profile that is available for plants.

This is one of the constant variables in the model to be applied for both water yield calculations, 1984 and 2022.

2.2.4. Root-Restricting Layer Depth

These data were downloaded from the Global Soil Information Grid platform provided by the International Soil Reference and Information Center (ISRIC) [9]. The information corresponding to the study area was taken and subsequently converted into a 10×10 m resolution and reprojected to the WGS 84/UTM zone 19S system coordinates, so that it was compatible with the other layers.

This is one of the constant variables in the model to be applied for both water yield calculations, 1984 and 2022.

2.2.5. Biophysical Parameters

The biophysical table (Table 3) was based on information from the FAO and recommendations were provided by the InVEST user manual.

Table 3. Biophysical table used for both years.

Type of Class of Land Use	Lucode	Lulc_veg	kc
IW	1	0	1
F	2	1	0.9
OS1	3	1	0.55
HAA	4	1	0.85
UF	5	0	0.15
OS2	6	1	0.6

Note: Sources: FAO, [21].

2.2.6. Zhang Parameter

The Zhang parameter was determined by the following equation:

$$Z = 0.2 \times N \quad (2)$$

where N is the number of rainfall events in a year which are over 1 mm [20].

For both 1984 and 2022, the number of rainfall events (higher than 1 mm) were 18. This translates into $Z = 3.6$, which is rounded to 4 when applying it to the model.

2.3. The InVEST Annual Water Yield Model

The InVEST annual water yield model estimates the relative water contributions from different parts of a landscape or study area, offering varied information about how changes in land use patterns affect annual surface water yield and hydropower production [21].

The equation used to determine the annual water yield for each landscape pixel is as follows:

$$Y(x) = \left(1 - \frac{AET(x)}{P(x)}\right) \times P(x) \quad (3)$$

where $AET(x)$ is the actual annual evapotranspiration for pixel x and $P(x)$ is the annual precipitation at pixel x .

For vegetated land use/cover (LULC), the evapotranspiration portion of water balance $AET(x)/P(x)$ is based on a Budyko curve expression proposed by [4,53]:

$$\frac{AET(x)}{P(x)} = 1 + \frac{PET(x)}{P(x)} - \left[1 + \left(\frac{PET(x)}{P(x)} \right)^w \right]^{\left(\frac{1}{w}\right)} \quad (4)$$

where $PET(x)$ is the potential evapotranspiration, defined by the following equation:

$$PET(x) = Kc(\uparrow x) \times ETo(x) \quad (5)$$

where $Eto(x)$ is represented by the referential evapotranspiration for pixel x , and Kc represents the vegetation evapotranspiration coefficient associated with each land use class for each pixel x .

$W(x)$ is a non-physical parameter that characterizes the climatic properties of soils, and it is defined by the following equation:

$$w(x) = Z \times \frac{AWC(x)}{P(x)} + 1.25 \quad (6)$$

where $AWC(x)$ is the volumetric water content available for plants expressed in millimeters and Z is the Zhang coefficient defined by the number of annual precipitation events in the study area.

For other types of land use, such as open water, urban areas and wetlands, the actual evapotranspiration value comes directly from the reference evapotranspiration $ETo(x)$ and has a maximum limit defined by precipitation:

$$AET(x) = \text{Min}(Kc(\uparrow x) \times ETo(x), P(x)) \quad (7)$$

where $ETo(x)$ represents the reference evapotranspiration and Kc is the evapotranspiration factor for each type of land use class.

2.4. Validation of Land Use Raster (Precision Analysis)

To validate the land use raster, the precision analysis method using polygons was applied. Here, polygons were created manually along the satellite image raster, and then, after being classified, and a precision tool was applied to them in the post processing section of the QGIS SCP plugin. The precision tool compares the generated and classified polygons for each class with the LULC raster. As a result, a table of accuracy analysis was obtained for each year. This table shows the values of SE (standard error), SE area, 95%CI (confidence interval) area, PA (producer's accuracy), UA (user's accuracy) and Kappa hat for each LULC class, as well as the total precision and kappa classification in the raster.

This method was employed because the LULC rasters were created not only based on the satellite images but also in the Arequipa's 2017 ecological and economical zoning to identify land use classes.

3. Results

3.1. Results of the Model

The results of the model were mainly influenced by different precipitation changes, evapotranspiration, and land use in time (Figure 3).

As observed in Figure 3, water yield is mainly influenced by the annual average precipitation, which represents the amount of water that reaches the study area through nature, while soil cover is the factor that dictates how much water from precipitation is stored. In 1984, there was more precipitation than in 2022, and therefore, there was higher water yield. However, in 2022, there was greater evapotranspiration by land use class. The amount of surface area that these land use classes covered in the study years selected can be expressed in numbers (Table 4).

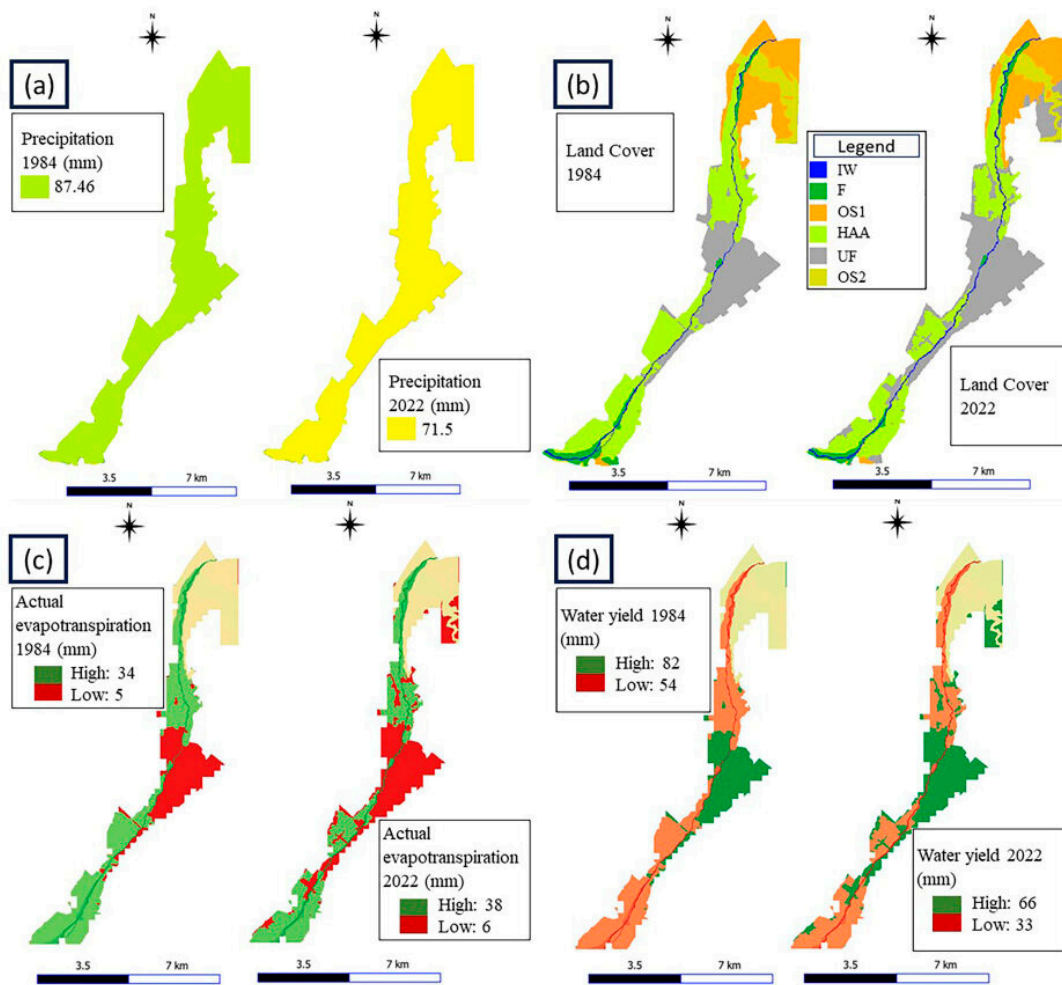


Figure 3. Precipitation (a), land cover (b), actual evapotranspiration (c) and water yield (d) in the urban section of Chili River in the years 1984 and 2022.

Table 4. Total area of land use classes and their percentage of change in the urban section of Chili River in 1984 and 2022.

Land Use Classes/Land Cover	Area				Percentage of Change
	1984		2022		
	Km ²	%	Km ²	%	
IW	0.657	2.53%	0.535	2.09%	−18.6%
F	1.181	4.56%	0.856	3.35%	−27.5%
OS1	5.227	20.16%	4.390	17.18%	−16.0%
HAA	10.360	39.96%	8.326	32.58%	−19.6%
UF	6.47	24.95%	9.953	38.94%	+53.8%
OS2	2.032	7.84%	1.497	5.86%	−26.3%

3.2. Land Use

These percentages of land use can be better observed in Figure 4.

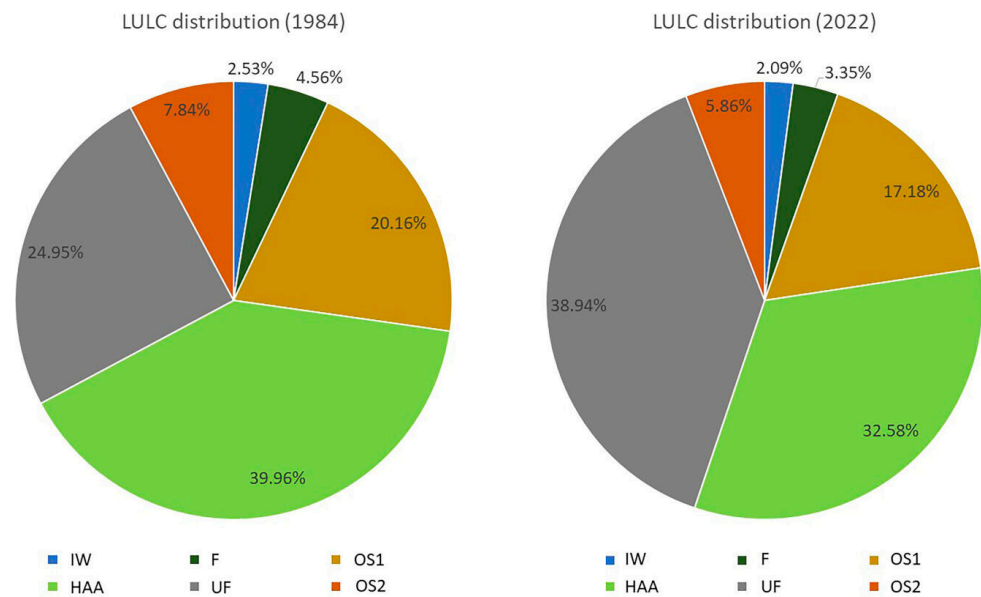


Figure 4. Distribution of land use in the study area in 1984 and 2022.

It is important to note that while in 1984, the agricultural area occupied most of the study area, in 2022, the urban area (UF) became the one occupying most of the study area, as shown in Table 4. This denotes a change in land use between 1984 and 2022 which has shown an accelerated urbanization process, where all types of land use, except the urban area which has increased more than 50%, have been significantly reduced.

In 1984, water yield was $1.74 \times 10^6 \text{ m}^3$ (1,743,414 m^3) or 67 mm, but in 2022, it was $1.32 \times 10^6 \text{ m}^3$ (1,323,792 m^3) or 51 mm. In Table 5, the effect LULC change on evapotranspiration and consequently on water yield can be observed.

Table 5. Water yield expressed in mm and m^3 for each land use class in the urban section of Chili River in 1984 and 2022.

Types of Land Use Classes/ Land Cover	Water Yield (m^3)				Actual Evapotranspiration (m^3)			
	1984		2022		1984		2022	
	mm	m^3	mm	m^3	mm	m^3	mm	m^3
IW	54	35,478	33	17,655	33	21,681	38	20,330
F	57	67,317	37	31,672	30	35,430	34	29,104
OS1	69	360,663	50	219,500	18	94,086	21	92,190
HAA	59	611,240	39	324,714	28	290,080	32	266,432
UF	82	530,540	66	656,898	5	32,350	6	59,718
OS2	68	138,176	49	73,353	20	40,640	22	32,934
Total		1,743,414		1,323,792		514,267		500,708

3.3. Water Yield and Actual Evapotranspiration

This change in water yield and evapotranspiration can be better observed in Figure 5.

The water yield in 1984 was higher than the one calculated in 2022, as shown in Table 3. However, water yield per cubic meter in the urban area increased despite a lower amount of annual precipitation. This represents the land use class with the highest water yield, while the river (IW), the riparian forest (F) and the agricultural area (HAA) are the classes with the lowest values. The urban area (UF) occupied 50% of the total water yield of the study area in 2022, despite not even occupying 40% of the area. In addition, all of the other values of the remaining land use classes have been reduced.

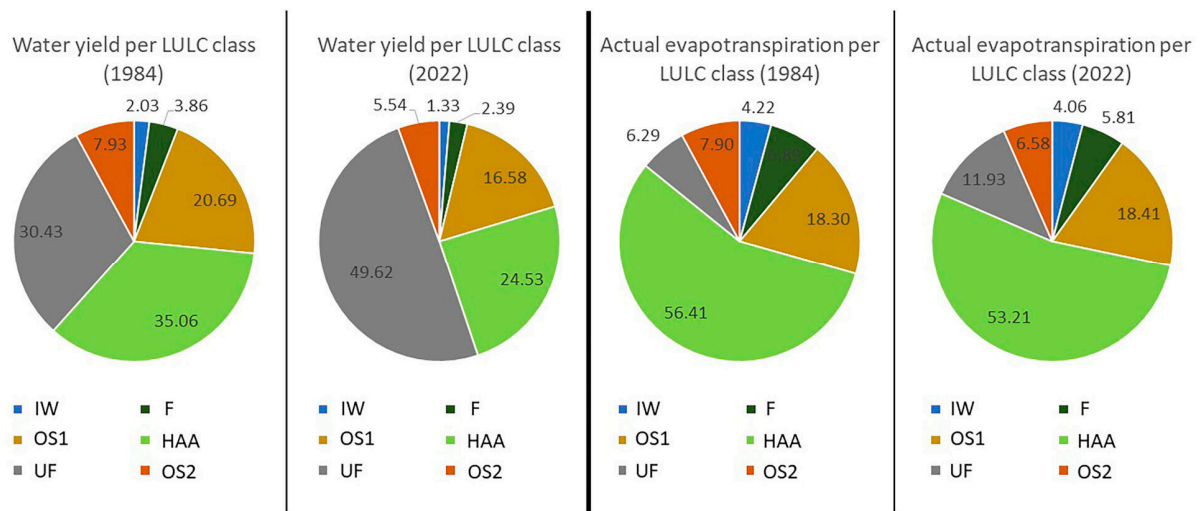


Figure 5. Distribution of water yield and actual evapotranspiration in the study area in 1984 and 2022.

Regarding the actual evapotranspiration (Table 5), it is observed that there was more evapotranspiration per millimeter in each land use class, which can be explained by a temperature increase. Contrary to what happens with water yield, the urban area (UF) is the land use class with the least evapotranspiration in both years, while the river (IW), riparian forest (F) and agricultural area (HAA) are the classes with the highest evapotranspiration numbers. Despite the increase per millimeter in each land use class, evapotranspiration per cubic meters was decreased, which is due to the increase in the extension of the urban area. This is because although this type of land use has a low value in this parameter, in terms of cubic meters, it has almost doubled its percentage of total evapotranspiration losses in the study area. The analysis by cubic meters, with the agricultural area being one of the land use classes with the largest surface area in the study area and adding to the high value of its cultivation coefficient, explains why this area has the highest amount of water loss due to evapotranspiration, despite the riparian forest (F) having a higher loss rate per pixel. The land use classes with greater evapotranspiration presented lower water (per mm) and vice versa (Table 5), demonstrating that evapotranspiration is an important factor in the water yield loss and is associated to land use classes. The urban area is the land use class with the greatest effect on the results shown due to this factor.

3.4. LULC Validation

The validation test regarding the land use classes is represented in Table 6.

Table 6. Accuracy test for land use classes in the urban section of Chili River in 1984 and 2022.

Year	Accuracy	IW	F	OS1	HAA	UF	OS2
1984	SE	0.0004	0.0003	0.0004	0.0005	0.0003	0.0004
	SE area	9363	8837	11,072	11,842	8471	9590
	95%CI area	18,352	17,320	21,701	23,211	16,603	18,796
	PA (%)	74.03	86.97	95.89	97.49	95.18	75.34
	UA (%)	69.62	80.07	86.35	95.46	99.02	97.86
	Kappa hat	0.6888	0.7921	0.8332	0.9255	0.9868	0.9762
	OA (%)				93.35		
	Kappa Classification				0.9091		

Table 6. Cont.

Year	Accuracy	IW	F	OS1	HAA	UF	OS2	
2022	SE	0.0002	0.0002	0.0002	0.0003	0.0002	0.0002	
	SE area	5993	4681	5644	7661	6110	5654	
	95%CI area	11,747	9174	11,063	15,015	11,975	11,081	
	PA (%)	99.47	90.65	96.23	97.33	98.29	92.90	
	UA (%)	84.95	95.86	97.85	98.85	98.13	88.99	
	Kappa hat	0.8454	0.9571	0.9739	0.9827	0.9702	0.8833	
	OA (%)				97.30			
	Kappa Classification				0.9623			

Notes: Area unit = m²; SE = standard error; CI = confidence interval; PA: producer's accuracy; UA: user's accuracy; OA: overall accuracy.

In 2022, the validation test was more accurate for both the land use class average and for each land use class compared to the validation test in 1984; this was due to the difference between base satellite image resolutions, where land use classes with a smaller area were more affected by the validation test in the year 1984. In this way, categories with a larger area had a better validation percentage. The complete accuracy assessment tables that were obtained directly from the software are shown in Appendix A.

4. Discussion

Regarding the increase in urban area, a study carried out by [36,42] demonstrated that between the years 1984 and 2020, Arequipa city has expanded its urban zone by 208 km² (from 67.8 km² to 275.8 km²), with a decrease in green areas, especially those in the Northern Cone districts. The districts having to replace their green areas the most due to this growth are Cayma, Cerro Colorado, Mollebaya, Quequeña, Sachaca, Socabaya and Yura. These results are consistent with those represented in Table 1.

The results regarding water yield (Table 3) agree with previous studies which demonstrated that land covered with more vegetation tends to have less water yield because of the water-absorbing property of the soil [9,40]. However, the water yield increase does not always have a positive effect on the study area, but its effect depends on the soil properties and type of soil. A study carried out by [9] indicated that the water yield produced by bare land cover is mainly produced in the form of surface runoff, which may have an impact on the decrease in infiltration capacity and the increase in runoff, erosion and sedimentation. On the other hand, the main effects on the changes in land use/cover on water yield are hydrological cycle processes and changes in water quality [54]. These contributions encourage caution to be taken when interpreting the results obtained here.

Actual evapotranspiration is a factor that reduces water yield and is determined by climatic parameters such as solar radiation, precipitation, temperature and land use [55]. From the land use classes, it can be seen that the urban area is the class with the highest water yield. This can be explained due to less evapotranspiration present here than in the other remaining areas. Studies conducted by [7,9] also showed a higher amount of water yield in areas without vegetation due to this characteristic. In the study carried out by [56], they evaluated the global impacts of native vegetation conversion into agricultural lands with respect to the water yield and concluded that the increase in cropland and pastures during the last 300 years, and the decrease in forest lands, decreases evapotranspiration [57]. This can be corroborated in this study by observing that the evapotranspiration value of the riparian forest (F) representing native vegetation is greater than the one in the agricultural area.

Studies analyzing water yield in different places have in common the fact that they apply this model to larger study areas [9,20,40] compared to our study case, which allows them to interpolate the precipitation data and create maps of this parameter with ranges and variations that our study could not apply due to the lack of meteorological stations

that produce more data by measuring this parameter, the only available station being the Pampilla station.

Several studies have carried out sensitivity analyses [3,58] on the model's results which allows them to be solid and reliable, comparing them to real values. Additionally, scenario analysis such as in the study carried out by [40] allows for the prediction of water yield behavior in future years. It is also advisable to perform such analyses in case this study is expanded in the future and there are physical measurements at the same site that can corroborate the model data.

In line with the study by [45], the study carried out by [59] demonstrates that this model can be useful to predict damage to natural ecosystems, such as floods caused by seasonal rain in desert areas, pointing out that green infrastructure to protect the natural ecosystem services is required. The InVEST WY model is also associated with hydroelectric production capacity, which is why it can be useful for future projects and investments that decide to take advantage of the water yield of the study area to produce energy.

The InVEST model assumes that water yield of a pixel reaches a point such that the model does not distinguish between surface water and groundwater [40,58]. Additionally, the model does not consider sub-annual patterns of water delivery timing such as seasonal or sub-seasonal variability, as well as water flow distribution [21]. However, it is easy to use, and it is reliable in terms of its results, as observed in Table 2, which is supported by the studies carried out by [18] in Indonesia, and Iran [59].

Although water yield increases with urban growth due to the reduction in evapotranspiration, it can also represent a loss of water resources due to water runoff that flows straight to the sewers that reach the city drain. Such an ES should be used by redirecting this water runoff toward the main channel of the river, where this water retention can be taken advantage of with the type of vegetation. In the same way, sustainable eco zoning could be implemented supported by governance policies and urban planning for the creation of green areas that contain vegetation that can improve WY [60].

Regarding the limitations of the model, the InVEST water yield model requires simpler inputs compared to other hydrological models, one of which is the Soil and Water Assessment Tool (SWAT). This causes InVEST to be more highly recommended for use in areas with limited data [9], such as for this case study, which was limited by the lack of meteorological information, since data from only one meteorological station were available for the study area. In addition, it is noted that despite the good performance, this simplification and limitation might affect the accuracy of the modeled water yield values, including its inability to account for interior intra-annual variation [20]. In addition to this, other complementary studies related to the topographic and geological configuration of basins [39], hydrogeomorphology and geodiversity [2] could be carried out.

Using the WY model, eco zoning could be implemented that establishes clear limits for the urban growth of the city, where the creation of areas of vegetation cover is promoted in order to allow for the improvement in this ES [60]. This, accompanied by ecological education processes, would allow for the generation of successful ecological governance policies and sustainable urban growth.

5. Conclusions

The application of the InVEST model in the study area resulted in 1,743,414 cubic meters of water yield for 1984 versus 1,323,792 cubic meters for 2022. It was determined that land use changes related to evapotranspiration and runoff cause a considerable change in the total WY of a basin, although the average annual precipitation is the most influential factor on the WY.

The change in land use caused by the constant acceleration of the urbanization process that Arequipa city has experienced in the last 40 years has been reflected in a negative WY increase, where evapotranspiration and infiltration are reduced, causing WY in urban zones to become more prone to produce superficial runoff and even flood risk.

The river area did not have great impact on these results due to the small area it occupies compared to the others. However, it is the least affected one in terms of area because

of the urbanization process. The agricultural land use showed the greatest reduction over time, while the urban land use had the greatest increase. Cardonal area (OS1), Puyal area (OS2) and riparian forest (F) were also reduced due to the urbanization effects, but to a lesser extent than the agricultural area.

The simplicity of the InVEST model’s requirements allows it to be applicable to study areas where there is limited information or data. Nevertheless, despite the good performance of the model, this simplification and limitation might affect the accuracy of the modeled water yield values.

The InVEST water yield model requires simpler inputs compared to other hydrological models, one of which is the Soil and Water Assessment Tool (SWAT). This causes InVEST to be more highly recommended for use in areas with limited data [9], such as for this case study, which was limited by the lack of meteorological information, since only one meteorological reference station was available for the study area.

Even though the data inputs of the model are reliable, further studies or in situ validation tests are recommended to corroborate the results of the InVEST model.

The results of this study are intended to serve water resource managers, landscape planners and political decision makers. Thus, the model will allow for the planning of sustainable urban growth and the adequate management of water resources in Arequipa city and can be extended to other arid regions.

Author Contributions: Conceptualization, L.C.-V. and A.C.-M.; methodology, L.C.-V., K.V.-C. and B.C.-P.; software, L.C.-V., K.V.-C. and B.C.-P.; validation, L.C.-V. and B.C.-P.; formal analysis, L.C.-V.; investigation: L.C.-V., K.V.-C., C.I.-R., B.C.-P., A.O. and A.C.-M.; resources, A.C.-M.; data curation, L.C.-V. and B.C.-P.; writing-review and editing, L.C.-V., K.V.-C., C.I.-R., B.C.-P., A.O. and A.C.-M.; visualization, L.C.-V., K.V.-C. and C.I.-R.; supervision, C.I.-R., B.C.-P., A.O. and A.C.-M.; project administration, C.I.-R. and A.C.-M.; funding acquisition, C.I.-R. and A.C.-M. All authors have read and agreed to the published version of the manuscript.

Funding: The APC was funded by Universidad Católica de Santa María.

Data Availability Statement: The original contributions presented in the study are included in the article, further inquiries can be directed to the corresponding authors.

Conflicts of Interest: The authors declare no conflicts of interest.

Appendix A. Complete Accuracy Assessment of the LULC Rasters

V_Classified	1	2	3	4	5	6	Total
1	1265	59	0	348	145	0	1817
2	485	3408	55	235	0	73	4256
3	7	510	30985	52	0	4331	35885
4	114	254	784	57394	1575	0	60121
5	41	9	0	411	46757	0	47218
6	0	5	335	0	0	15550	15890
Total	1912	4245	32159	58440	48477	19954	165187

> AREA BASED ERROR MATRIX								
> Referencia								
V_Classified	1	2	3	4	5	6	Area	Wi
1	0.0176	0.0008	0.0000	0.0049	0.0020	0.0000	657700.0000	0.0253
2	0.0052	0.0364	0.0006	0.0025	0.0000	0.0008	1179000.0000	0.0454
3	0.0000	0.0029	0.1741	0.0003	0.0000	0.0243	5233500.0000	0.2016
4	0.0008	0.0017	0.0052	0.3817	0.0105	0.0000	10376400.0000	0.3998
5	0.0002	0.0000	0.0000	0.0022	0.2470	0.0000	6473100.0000	0.2494
6	0.0000	0.0000	0.0017	0.0000	0.0000	0.0767	2035000.0000	0.0784
Total	0.0238	0.0418	0.1816	0.3915	0.2595	0.1018	25954700.0000	
Area	618564	1085534	4712331	10160735	6734220	2643316	25954700	
SE	0.0004	0.0003	0.0004	0.0005	0.0003	0.0004		
SE area	9363	8837	11072	11842	8471	9590		
95% CI area	18352	17320	21701	23211	16603	18796		
PA [%]	74.0250	86.9698	95.8948	97.4904	95.1840	75.3393		
UA [%]	69.6203	80.0752	86.3453	95.4641	99.0237	97.8603		
Kappa hat	0.6888	0.7921	0.8332	0.9255	0.9868	0.9762		

Precisión total [%] =93.3471
 Clasificación Kappa =0.9091

Area unit = metre^2
 SE = standard error
 CI = confidence interval
 PA = producer's accuracy
 UA = user's accuracy

Figure A1. Accuracy assessment for LULC classes in 1984.

V_Classified	1	2	3	4	5	6	Total
1	1930	73	0	260	9	0	2272
2	15	5167	69	77	0	62	5390
3	0	0	37520	144	86	595	38345
4	4	191	44	65990	530	0	66759
5	5	270	89	831	72082	178	73455
6	0	0	1093	3	177	10285	11558
Total	1954	5701	38815	67305	72884	11120	197779

> AREA BASED ERROR MATRIX								
> Referencia								
V_Classified	1	2	3	4	5	6	Area	Wi
1	0.0261	0.0010	0.0000	0.0035	0.0001	0.0000	792700.0000	0.0307
2	0.0001	0.0321	0.0004	0.0005	0.0000	0.0004	865200.0000	0.0335
3	0.0000	0.0000	0.1690	0.0006	0.0004	0.0027	4463100.0000	0.1727
4	0.0000	0.0009	0.0002	0.3250	0.0026	0.0000	8499100.0000	0.3288
5	0.0000	0.0014	0.0005	0.0043	0.3689	0.0009	9716300.0000	0.3759
6	0.0000	0.0000	0.0055	0.0000	0.0009	0.0520	1510200.0000	0.0584
Total	0.0262	0.0354	0.1756	0.3339	0.3729	0.0560	25846600.0000	
Area	676955	914904	4538340	8631346	9638437	1446618	25846600	
SE	0.0002	0.0002	0.0002	0.0003	0.0002	0.0002	0.0002	
SE area	5993	4681	5644	7661	6110	5654		
95% CI area	11747	9174	11063	15015	11975	11081		
PA [%]	99.4714	90.6547	96.2263	97.3336	98.9236	92.8971		
UA [%]	84.9472	95.8627	97.8485	98.8481	98.1308	88.9860		
Kappa hat	0.8454	0.9571	0.9739	0.9827	0.9702	0.8833		

Precisión total [%] =97.3033
Clasificación Kappa =0.9623

Area unit = metre^2
SE = standard error
CI = confidence interval
PA = producer's accuracy
UA = user's accuracy

Figure A2. Accuracy assessment for LULC classes in 2022.

References

- Liao, K.-H. The socio-ecological practice of building blue-green infrastructure in high-density cities: What does the ABC Waters Program in Singapore tell us? *Socio-Ecol. Pract. Res.* **2019**, *1*, 67–81. [\[CrossRef\]](#)
- Ollero, A. *Hidrogeomorfología y Geodiversidad: El Patrimonio Fluvial*, 1st ed.; Centro de Documentación del Agua y del Medio Ambiente, Ayuntamiento de Zaragoza: Zaragoza, Spain, 2017; Volume 1.
- Valencia, J.B.; Guryanov, V.V.; Mesa-Diez, J.; Tapasco, J.; Gusarov, A.V. Assessing the Effectiveness of the Use of the InVEST Annual Water Yield Model for the Rivers of Colombia: A Case Study of the Meta River Basin. *Water* **2023**, *15*, 1617. [\[CrossRef\]](#)
- Ollero, A.; García, J.H.; Ibisate, A.; Sánchez-Fabre, M. Updated knowledge on floods and risk management in the Middle Ebro River: The “Anthropocene” context and river resilience. *Cuad. Investig. Geográfica* **2021**, *47*, 73–94. [\[CrossRef\]](#)
- Magdaleno, F.; Cortés, F.; Martín, B. Infraestructuras Verdes y Azules: Estrategias de Adaptación y Mitigación Ante El Cambio Climático. Green and Blue Infrastructures: Adaptation and Mitigation Strategies to Climate Change. *Rev. Digit. Cedex* **2018**, *191*, 105–112.
- Wang, X.; Liu, G.; Lin, D.; Lin, Y.; Lu, Y.; Xiang, A.; Xiao, S. Water yield service influence by climate and land use change based on InVEST model in the monsoon hilly watershed in South China. *Geomat. Nat. Hazards Risk* **2022**, *13*, 2024–2048. [\[CrossRef\]](#)
- Geng, X.; Wang, X.; Yan, H.; Zhang, Q.; Jin, G. Land Use/Land Cover Change Induced Impacts on Water Supply Service in the Upper Reach of Heihe River Basin. *Sustainability* **2015**, *7*, 366–383. [\[CrossRef\]](#)
- Campo, C.C.; Alfonso, W.H. Relationship between the Processes of Urbanization and International Trade, and its Impact on Urban Sustainability. *Cuad. Vivienda Urban.* **2018**, *11*, 1–10. [\[CrossRef\]](#)
- Ningrum, A.; Setiawan, Y.; Tarigan, S.D. Annual Water Yield Analysis with InVEST Model in Tesso Nilo National Park, Riau Province. *IOP Conf. Ser. Earth Environ. Sci.* **2022**, *950*, 012098. [\[CrossRef\]](#)
- Brauman, K.A. Hydrologic ecosystem services: Linking ecohydrologic processes to human well-being in water research and watershed management. *WIREs Water* **2015**, *2*, 345–358. [\[CrossRef\]](#)
- Cudennec, C.; Leduc, C.; Koutsoyiannis, D. Dryland hydrology in Mediterranean regions—A review. *Hydrol. Sci. J.* **2007**, *52*, 1077–1087. [\[CrossRef\]](#)
- Long, C.; Gaudi, X.I.E.; Changshun, Z.; Sha, P.E.I.; Na, F.A.N.; Liqiang, G.E.; Caixia, Z. Modelling Ecosystem Water Supply Services across the Lancang River Basin. *J. Resour. Ecol.* **2011**, *2*, 322. [\[CrossRef\]](#)
- Jobbágy, E.G.; Acosta, A.M.; Nosetto, M.D. Rendimiento hídrico en cuencas primarias bajo pastizales y plantaciones de pino de las sierras de Córdoba (Argentina). *Ecol. Austral.* **2013**, *23*, 87–96. [\[CrossRef\]](#)
- Lovera Pons, V.; Roldán Aragón, I.E.; Sánchez Robles, J.; Torres Lima, P. Evaluación del servicio ecosistémico de rendimiento hídrico entre los años de 1994 y 2016 en el municipio de Valle de Bravo, estado de México. *Papeles Geogr.* **2018**, *64*, 93–113. [\[CrossRef\]](#)
- Elliott, K.J.; Caldwell, P.V.; Brantley, S.T.; Miniati, C.F.; Vose, J.M.; Swank, W.T. Water yield following forest–grass–forest transitions. *Hydrol. Earth Syst. Sci.* **2017**, *21*, 981–997. [\[CrossRef\]](#)
- Jobbágy, E. Servicios hídricos de los ecosistemas y su relación con el uso de la tierra en la llanura Chaco-Pampeana. In *Valoración de Servicios Ecosistémicos. Conceptos, Herramientas y Aplicaciones Para el Ordenamiento Territorial*; Ediciones INTA: Buenos Aires, Argentina, 2011; pp. 163–183.

17. Yu, J.; Yuan, Y.; Nie, Y.; Ma, E.; Li, H.; Geng, X. The Temporal and Spatial Evolution of Water Yield in Dali County. *Sustainability* **2015**, *7*, 6069–6085. [[CrossRef](#)]
18. Yudistiro; Kusratmoko, E.; Semedi, J.M. Water Availability in Patuha Mountain Region Using InVEST Model “Hydropower Water Yield”. In Proceedings of the 4th International Conference on Energy, Environment, Epidemiology and Information System, Semarang, Indonesia, 7–8 August 2019; Volume 125, p. 01015.
19. Shirmohammadi, B.; Malekian, A.; Salajegheh, A.; Taheri, B.; Azarnivand, H.; Malek, Z.; Verburg, P.H. Impacts of future climate and land use change on water yield in a semiarid basin in Iran. *Land Degrad. Dev.* **2020**, *31*, 1252–1264. [[CrossRef](#)]
20. Yin, G.; Wang, X.; Zhang, X.; Fu, Y.; Hao, F.; Hu, Q. InVEST Model-Based Estimation of Water Yield in North China and Its Sensitivities to Climate Variables. *Water* **2020**, *12*, 1692. [[CrossRef](#)]
21. Sharp, R.; Chaplin-Kramer, R.; Wood, S.; Guerry, A.; Tallis, H.; Ricketts, T.; Nelson, E.; Ennaanay, D.; Wolny, S.; Olwero, N.; et al. *InVEST User’s Guide*; University of Minnesota: Minneapolis, MN, USA, 2018.
22. Lu, N.; Sun, G.; Feng, X.; Fu, B. Water yield responses to climate change and variability across the North–South Transect of Eastern China (NSTEC). *J. Hydrol.* **2013**, *481*, 96–105. [[CrossRef](#)]
23. Ouyang, Z.; Zhu, C.; Yang, G.; Xu, W.; Zheng, H.; Zhang, Y.; Xiao, Y. Gross ecosystem product: Concept, accounting framework and case study. *Acta Ecol. Sin.* **2013**, *33*, 6747–6761. [[CrossRef](#)]
24. Ma, Y.; Zheng, M.; Zheng, X.; Huang, Y.; Xu, F.; Wang, X.; Liu, J.; Lv, Y.; Liu, W. Land Use Efficiency Assessment under Sustainable Development Goals: A Systematic Review. *Land* **2023**, *12*, 894. [[CrossRef](#)]
25. Benra, F.; De Frutos, A.; Gaglio, M.; Álvarez-Garretón, C.; Felipe-Lucia, M.; Bonn, A. Mapping water ecosystem services: Evaluating InVEST model predictions in data scarce regions. *Environ. Model. Softw.* **2021**, *138*, 104982. [[CrossRef](#)]
26. Babbar, D.; Areendran, G.; Sahana, M.; Sarma, K.; Raj, K.; Sivadas, A. Assessment and prediction of carbon sequestration using Markov chain and InVEST model in Sariska Tiger Reserve, India. *J. Clean. Prod.* **2021**, *278*, 123333. [[CrossRef](#)]
27. Jiang, W.; Deng, Y.; Tang, Z.; Lei, X.; Chen, Z. Modelling the potential impacts of urban ecosystem changes on carbon storage under different scenarios by linking the CLUE-S and the InVEST models. *Ecol. Model.* **2017**, *345*, 30–40. [[CrossRef](#)]
28. Choudhary, A.; Deval, K.; Joshi, P.K. Study of habitat quality assessment using geospatial techniques in Keoladeo National Park, India. *Environ. Sci. Pollut. Res.* **2021**, *28*, 14105–14114. [[CrossRef](#)]
29. Caro, C.; Marques, J.C.; Cunha, P.P.; Teixeira, Z. Ecosystem services as a resilience descriptor in habitat risk assessment using the InVEST model. *Ecol. Indic.* **2020**, *115*, 106426. [[CrossRef](#)]
30. Yang, X.; Guo, B.; Lu, Y.; Zhang, R.; Zhang, D.; Zhen, X.; Chen, S.; Wu, H.; Wei, C.; Yang, L.; et al. Spatial–temporal evolution patterns of soil erosion in the Yellow River Basin from 1990 to 2015: Impacts of natural factors and land use change. *Geomat. Nat. Hazards Risk* **2021**, *12*, 103–122. [[CrossRef](#)]
31. Kadaverugu, A.; Nageshwar Rao, C.; Viswanadh, G.K. Quantification of flood mitigation services by urban green spaces using InVEST model: A case study of Hyderabad city, India. *Model. Earth Syst. Environ.* **2021**, *7*, 589–602. [[CrossRef](#)]
32. Quagliolo, C.; Comino, E.; Pezzoli, A. Experimental Flash Floods Assessment Through Urban Flood Risk Mitigation (UFRM) Model: The Case Study of Ligurian Coastal Cities. *Front. Water* **2021**, *3*, 663378. [[CrossRef](#)]
33. Belete, M.; Deng, J.; Abubakar, G.A.; Teshome, M.; Wang, K.; Woldetsadik, M.; Zhu, E.; Comber, A.; Gudo, A. Partitioning the impacts of land use/land cover change and climate variability on water supply over the source region of the Blue Nile Basin. *Land Degrad. Dev.* **2020**, *31*, 2168–2184. [[CrossRef](#)]
34. Wamucii, C.N.; van Oel, P.R.; Ligtenberg, A.; Gathenya, J.M.; Teuling, A.J. Land use and climate change effects on water yield from East African forested water towers. *Hydrol. Earth Syst. Sci.* **2021**, *25*, 5641–5665. [[CrossRef](#)]
35. Ronchi, S.; Salata, S.; Arcidiacono, A. Which urban design parameters provide climate-proof cities? An application of the Urban Cooling InVEST Model in the city of Milan comparing historical planning morphologies. *Sustain. Cities Soc.* **2020**, *63*, 102459. [[CrossRef](#)]
36. Pessacg, N.; Flaherty, S.; Brandizi, L.; Solman, S.; Pascual, M. Getting water right: A case study in water yield modelling based on precipitation data. *Sci. Total Environ.* **2015**, *537*, 225–234. [[CrossRef](#)]
37. Li, Y.; Piao, S.; Li, L.Z.X.; Chen, A.; Wang, X.; Ciais, P.; Huang, L.; Lian, X.; Peng, S.; Zeng, Z.; et al. Divergent hydrological response to large-scale afforestation and vegetation greening in China. *Sci. Adv.* **2018**, *4*, eaar4182. [[CrossRef](#)] [[PubMed](#)]
38. Zhang, L.; Cheng, L.; Chiew, F.; Fu, B. Understanding the impacts of climate and landuse change on water yield. *Curr. Opin. Environ. Sustain.* **2018**, *33*, 167–174. [[CrossRef](#)]
39. Canqiang, Z.; Wenhua, L.; Biao, Z.; Moucheng, L. Water Yield of Xitiao River Basin Based on InVEST Modeling. *J. Resour. Ecol.* **2012**, *3*, 50–54. [[CrossRef](#)]
40. Lian, X.; Qi, Y.; Wang, H.; Zhang, J.; Yang, R. Assessing Changes of Water Yield in Qinghai Lake Watershed of China. *Water* **2020**, *12*, 11. [[CrossRef](#)]
41. Zeballos, C. *Atlas Ambiental de Arequipa*; Vicerrectorado de Investigación de la Universidad Católica de Santa María; Neo Cromatika: Arequipa, Peru, 2020; Volume 1.
42. Arela Bobadilla, R.; Riesco Lind, G.; Chávez Contreras, G. *Una Mirada a la Expansión de la Ciudad de Arequipa en Los Últimos 40 Años | Entradas UCSP: Informes CEEE*; Informe del Centro de Estudios en Economía y Empresa; Universidad Católica San Pablo: Arequipa, Peru, 2021; pp. 1–30.
43. Wang, K.; Li, S.; Zhu, Z.; Gao, X.; Li, X.; Tang, W.; Liang, J. Identification of priority conservation areas based on ecosystem services and systematic conservation planning analysis. *Environ. Sci. Pollut. Res.* **2023**, *30*, 36573–36587. [[CrossRef](#)] [[PubMed](#)]

44. ANA Consejo de Recursos Hídricos de Cuenca Quilca—Chili. Available online: <https://www.ana.gob.pe/consejo-de-cuenca/quilca-chili/portada> (accessed on 22 January 2024).
45. Iruri Ramos, C.P.; Chanove Manrique, A.; Vilca Campana, K.; Carrasco Valencia, L.; Cárdenas Pillco, B.E. Servicios ecosistémicos de la infraestructura azul-verde para la adaptación y mitigación del cambio climático: Caso del tramo urbano del Río Chili, Arequipa (Perú). In *Ríos Urbanos en Iberoamérica: Casos, Contextos y Experiencias*; Edições Universitárias Lusófonas: Lisbon, Portugal, 2023; Volume 6, pp. 203–223.
46. Duran Vian, F.; Pons Izquierdo, J.J.; Serrano Martínez, M. ¿Qué es un río urbano? Propuesta metodológica para su delimitación en España. *ACE Arquít. Ciudad Entorno* **2020**, *44*, 9035. [[CrossRef](#)]
47. Municipalidad Provincial de Arequipa. *Plan de Desarrollo Metropolitano de Arequipa 2016–2025*; Instituto Municipal de Planeamiento: Arequipa, Peru, 2015.
48. Oficina de Asesoría y Consultoría Ambiental—PROCHILI. *Plan de Gestión Ambiental de la Cuenca Metropolitana del Río Chili*; Editorial OACA: Arequipa, Peru, 2002.
49. Basak, S.M.; Hossain, M.S.; Tusznió, J.; Grodzińska-Jurczak, M. Social benefits of river restoration from ecosystem services perspective: A systematic review. *Environ. Sci. Policy* **2021**, *124*, 90–100. [[CrossRef](#)]
50. Asociación Peruana de la Energía Solar y del Ambiente (APES). *Aporte del Uso de la Energía Solar al Desarrollo de Arequipa en el siglo XXI*; Ministerio del Ambiente: Arequipa, Peru, 2015; p. 189.
51. MINAM. *Zonificación Ecológica y Económica de Arequipa*; Ministerio del Ambiente: Arequipa, Peru, 2018.
52. MINAM. *Mapa Nacional de Cobertura Vegetal: Memoria Descriptiva*; Dirección General de Evaluación, Valoración y Financiamiento del Patrimonio Natural: Lima, Peru, 2015.
53. Fu, B.P. On the Calculation of the Evaporation from Land Surface. *Sci. Atmos. Sin.* **1981**, *5*, 23–31.
54. Che, X.; Jiao, L.; Qin, H.; Wu, J. Impacts of Climate and Land Use/Cover Change on Water Yield Services in the Upper Yellow River Basin in Maqu County. *Sustainability* **2022**, *14*, 10363. [[CrossRef](#)]
55. Droogers, P.; Allen, R.G. Estimating Reference Evapotranspiration Under Inaccurate Data Conditions. *Irrig. Drain. Syst.* **2002**, *16*, 33–45. [[CrossRef](#)]
56. Scanlon, B.R.; Jolly, I.; Sophocleous, M.; Zhang, L. Global impacts of conversions from natural to agricultural ecosystems on water resources: Quantity versus quality. *Water Resour. Res.* **2007**, *43*, 1–18. [[CrossRef](#)]
57. Ouyang, Y. New insights on evapotranspiration and water yield in crop and forest lands under changing climate. *J. Hydrol.* **2021**, *603*, 127192. [[CrossRef](#)]
58. Almeida, B.; Cabral, P. Water Yield Modelling, Sensitivity Analysis and Validation: A Study for Portugal. *ISPRS Int. J. Geo-Inf.* **2021**, *10*, 494. [[CrossRef](#)]
59. Darvishi, A.; Yousefi, M. Using water yield ecosystem services to assess water scarcity in a metropolitan arid environment in Qazvin region (Iran). *Pap. Regió Metrop. Barc. Territ. Estratègies Planejament* **2022**, *64*, 216–222.
60. Tian, S.; Wu, W.; Shen, Z.; Wang, J.; Liu, X.; Li, L.; Li, X.; Liu, X.; Chen, H. A cross-scale study on the relationship between urban expansion and ecosystem services in China. *J. Environ. Manag.* **2022**, *319*, 115774. [[CrossRef](#)]

Disclaimer/Publisher’s Note: The statements, opinions and data contained in all publications are solely those of the individual author(s) and contributor(s) and not of MDPI and/or the editor(s). MDPI and/or the editor(s) disclaim responsibility for any injury to people or property resulting from any ideas, methods, instructions or products referred to in the content.